

# Polarized Target Experiments at LHC

L. L. Pappalardo<sup>1,2</sup>, V. Carassiti<sup>2</sup>, G. Ciullo<sup>1,2</sup>, P. Di Nezza<sup>3</sup>, P. Lenisa<sup>1,2</sup>, S. Mariani<sup>4</sup>,  
 M. Santimaria<sup>3</sup> and E. Steffens<sup>5</sup>

<sup>1</sup>*Dipartimento di Fisica e Scienze della Terra, Università di Ferrara, Italy*

<sup>2</sup>*INFN Ferrara, Italy*

<sup>3</sup>*INFN Laboratori Nazionali di Frascati, Frascati (Rome), Italy*

<sup>4</sup>*Dipartimento di Fisica, Università di Firenze and INFN Firenze, Italy*

<sup>5</sup>*Physics Dept., FAU Erlangen-Nürnberg, Erlangen, Germany*

*E-mail: pappalardo@fe.infn.it*

(Received December 24, 2021)

A polarized gaseous target, operated in combination with the high-energy, high-intensity LHC beams and a highly performing LHC particle detector, has the potential to open new physics frontiers and to deepen our understanding of the intricacies of the strong interaction in the non-perturbative regime of QCD. Specifically, the LHCspin project aims to develop, in the next few years, innovative solutions and cutting-edge technologies to access spin physics in high-energy polarized fixed-target collisions using the LHCb detector. Given its forward geometry ( $2 < \eta < 5$ ), the LHCb spectrometer is, in fact, perfectly suitable to cope with the forward kinematics of these collisions. Furthermore, being designed and optimized for the detection of heavy hadrons, it will allow to probe the nucleon's structure by exploiting new probes, such as inclusive production of  $c$ - and  $b$ -hadrons, an ideal tool to access, e.g., the essentially unexplored spin-dependent gluon TMDs. This configuration, with center-of-mass energies ranging from 115 GeV in  $pp$  interactions to 72 GeV per nucleon in collisions with ion beams, will allow to explore the nucleon's internal dynamics at unique kinematic conditions, by covering a wide backward rapidity region, including the poorly explored high  $x$ -Bjorken and high  $x$ -Feynman regimes. This ambitious task poses its basis on the recent installation of SMOG2, a storage-cell based unpolarized gas target in front of the LHCb spectrometer. With the installation of the proposed polarized target system, LHCb will become the first experiment delivering simultaneously unpolarized beam-beam collisions at 14 TeV and both polarized and unpolarized beam-target collisions at center-of-mass energies of the order of 100 GeV. The status of the LHCspin project is presented along with a selection of physics opportunities.

**KEYWORDS:** nucleon structure, quark and gluon TMDs, polarized target, single spin asymmetry, fixed-target collisions, Large Hadron Collider

## 1. Introduction

Among the experiments running at the Large Hadron Collider (LHC), LHCb is at present the only one that can be operated also in fixed-target mode. The LHCb detector [1] is a general-purpose forward spectrometer specialized in detecting hadrons containing  $c$  and  $b$  quarks. It is fully instrumented in the  $2 < \eta < 5$  region with state-of-the-art particle detectors including a Vertex Locator (VELO), a tracking system, two Cherenkov detectors, electromagnetic and hadronic calorimeters and a muon detector. Figure 1 shows a scheme of the upgraded LHCb detector [2], which is currently being installed in view of the upcoming Run 3 of LHC, expected to start in 2022.

Fixed-target measurements at LHCb are possible since the installation of the SMOG (System for Measuring the Overlap with Gas) device [3] in 2011, enabling the injection of noble gases at a pressure of  $O(10^{-7})$  mbar in the beam pipe section crossing the VELO. While the original motivation for the SMOG system was to allow for precise luminosity measurements based on the beam-imaging

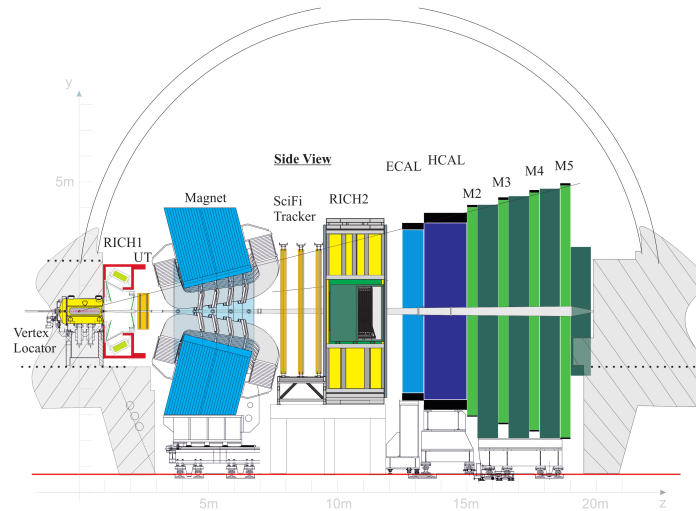


**Fig. 1.** The upgraded LHCb detector [2].

technique, a rich and unique fixed-target research program became possible during the LHC Run 2. Since 2015, several dedicated short SMOG runs have been performed at LHCb, exploiting only the LHC non-colliding bunches in order to avoid overlap with the beam-beam collisions. In particular p-He, p-Ar, p-Ne as well as Pb-Ar and Pb-Ne collisions have been performed at different beam energies, paving the way to a diverse physics program at unique kinematic conditions (see Sec. 2). Two analyses based on SMOG data, regarding anti-proton production in p-He collisions and charmed mesons production in p-He and p-Ar collisions, have been recently published [4, 5], whereas several different analyses of SMOG data are ongoing. Figure 2 shows the high-quality and low-background samples collected in just one week of dedicated SMOG runs during Run 2.

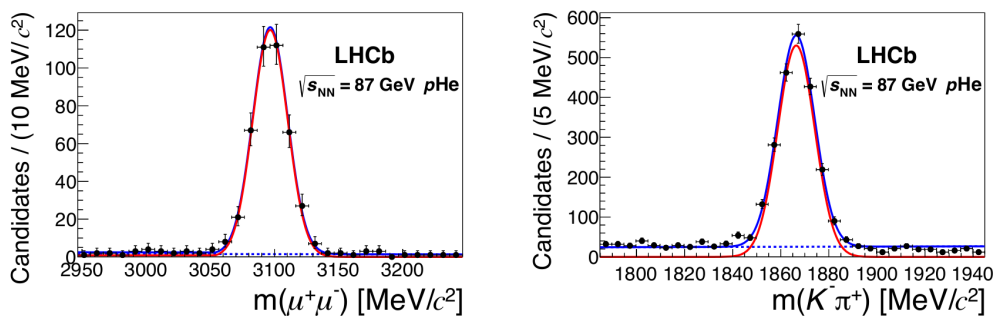


**Fig. 2.**  $J/\psi \rightarrow \mu^+\mu^-$  (left) and  $D^0 \rightarrow K^-\pi^+$  (right) SMOG samples from [5].

During the LHC Long Shutdown 2, the SMOG system has been upgraded with the installation, in front of the VELO, of an openable storage cell for the target gas, shown in Fig. 3. The use of the storage cell ensures target areal densities higher by up to two orders of magnitude with the same gas flow used for the original SMOG setup. The upgraded system, SMOG2 [6], to be operated from Run 3, also comprises a new and more sophisticated Gas Feed System (GFS). This new GFS will allow to measure the injected gas density (and so, in turn, the instantaneous luminosity) with a precision at the level of a few percents, and to inject several more gas species, including  $H_2$ ,  $D_2$ ,  $N_2$ ,  $O_2$ , Kr and Xe in addition to the three noble gases used with SMOG.

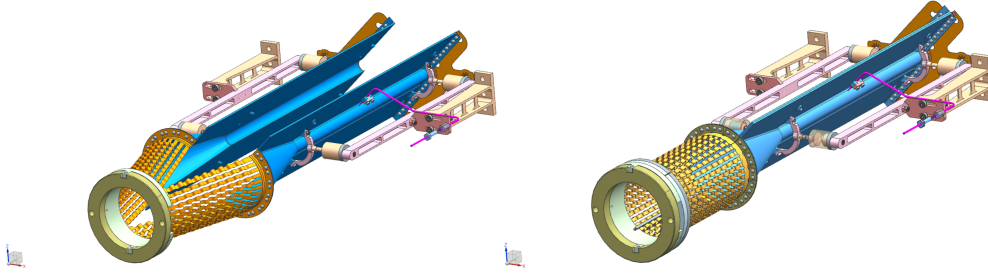


**Fig. 3.** The SMOG2 storage cell in the open (left) and closed (right) configuration.

The SMOG2 data will be collected with a novel reconstruction algorithm allowing simultaneous data taking of beam-gas and beam-beam collisions. Based on MC simulations, a very high tracking efficiency is expected in the beam-gas interaction region ( $-500 \text{ mm} < z < -300 \text{ mm}$ ), despite its upstream position with respect to the VELO. Furthermore, beam-gas and beam-beam vertices are well detached along the  $z$  coordinate, as shown in Fig. 4. The SMOG2 system will offer a rich physics program for the Run 3 and, at the same time, will allow to investigate the dynamics of the beam-target system, setting the basis for future developments.

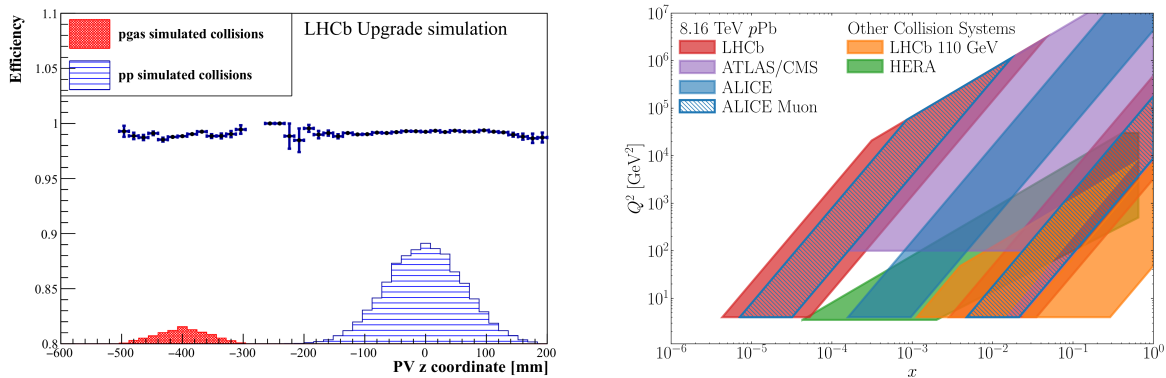


**Fig. 4.** Left: VELO track reconstruction efficiency for beam-gas (red) and beam-beam (blue) primary vertices [7]. Right: kinematic coverage of LHC fixed-target experiments (orange) compared to other experiments.

## 2. Fixed-target kinematics at LHC

During Run 2, LHC has delivered proton and lead beams with an energy of 6.5 TeV and 2.76 TeV per nucleon, respectively, with world highest intensity. Considering, for the Run 3, a 7 TeV proton beam, fixed-target beam-gas collisions will occur at a centre-of-mass energy per nucleon of  $\sqrt{s_{NN}} = 115 \text{ GeV}$ . This corresponds to a large Lorentz boost ( $\gamma \approx 60$ ) of the centre-of-mass in the laboratory system, resulting in a rapidity shift of  $\Delta y = y_{\text{Lab}} - y_{\text{CM}} \approx 4.8$ . At these conditions, the LHCb acceptance allows to cover backward and central rapidities in the centre-of-mass frame ( $-3 < y_{\text{CM}} < 0$ ). Such a coverage offers an unprecedented opportunity to investigate partons carrying a large fraction of the target nucleon momentum, i.e. large Bjorken- $x$  values, at intermediate  $Q^2$  (see Fig. 4 right), corresponding to large and negative Feynman- $x$  values ( $x_{\text{F}} \approx x_b - x_t$  where  $x_b$  and  $x_t$  are the Bjorken- $x$  values of the beam and target nucleon, respectively).

### 3. The LHCspin project

The LHCspin project [8] aims at extending the LHCb fixed-target program in Run 4 (expected to start in 2028) with the installation of a new-generation HERMES-like polarized gas target. The project, which also foresees the use of a storage cell for the target gas (polarized H or D), poses its basis on the recent installation of the SMOG2 storage cell in the LHC beam pipe, as well as on the well consolidated polarized-target technology and expertise, successfully employed at the HERMES experiment at HERA [9] and at the ANKE experiment at COSY [10]. Furthermore, dedicated studies have shown that the system will have a negligible interference with the LHC beam lifetime and the LHCb mainstream physics program and performance, and, thanks to the well displaced interaction regions, could run in parallel with the collider mode. Finally, the system will also allow to inject unpolarized gases (a-la SMOG2) and will benefit from both the LHC proton and heavy-ion beams and the state-of-the-art upgraded LHCb detector. All this will contribute to define a broad and ambitious physics program that ranges from the study of the nucleon structure, to the measurement of cold nuclear-matter effects, to the study of QGP observables and to astroparticle physics related to dark-matter searches. While many of these subjects are already at reach with the SMOG2 setup, the study of the spin-dependence of the nucleon structure in terms of quarks and gluons transverse-momentum-dependent parton distribution functions is only possible at LHC with the use of a polarized target, and represents the main physics objective of the project. A selection of physics opportunities accessible at LHCspin is presented in Sec. 3.1, while the experimental setup is discussed in Sec. 3.2.

#### 3.1 Physics case

The physics case of LHCspin covers three main areas: exploration of the wide physics potential offered by unpolarized gas targets, QGP and cold nuclear-matter studies in heavy-ion collisions, investigation of the nucleon spin structure. While the first two areas are common to SMOG2 and are presented in Ref. [11], the latter requires a polarized target and, as such, is unique of LHCspin. In the following only the physics cases that require a polarized target are discussed.

##### 3.1.1 Quark TMDs

Polarized quark and gluon distributions can be probed with LHCspin by means of proton collisions on polarized hydrogen and deuterium targets. Figure 5 shows the 5D Wigner distributions [12] which, upon integration on the transverse momentum, lead to the Generalized Parton Distributions (GPDs), while Transverse Momentum Dependent distributions (TMDs) are obtained when integrating over the transverse coordinate (impact parameter). Several leading-twist distributions, that can be probed using either unpolarized or transversely polarized targets, provide independent information on the spin structure of the nucleon.

The study of quark TMDs is among the main physics goals of LHCspin. Quark TMDs describe spin-orbit correlations inside the nucleon, making them indirectly sensitive to the unknown quark orbital angular momentum. Furthermore, they allow to construct 3D maps of the nucleon structure in the momentum space (*nucleon tomography*), as shown in Fig. 6 left. The golden process to get access to the quark TMDs in hadronic collisions is Drell-Yan (DY), where a quark and an anti-quark annihilate yielding a charged lepton pair (e.g.  $\mu^+\mu^-$ ) in the final state. At the LHC fixed-target kinematic conditions the dominant contribution to the process is the one where the anti-quark from the proton beam is probed at small- $x$ , and the quark from the target proton is probed at large- $x$ . By injecting unpolarized hydrogen one can get sensitivity to the unpolarized quark TMD,  $f_1(x, p_T^2)$ , and the Boer-Mulders function,  $h_1^\perp(x, p_T^2)$ , through the azimuthal dependence of the DY cross section:

$$d\sigma_{UU}^{DY} \propto f_1^{\bar{q}} \otimes f_1^q + \cos(2\phi) h_1^{\perp\bar{q}} \otimes h_1^{\perp q}, \quad (1)$$

where the symbol  $\otimes$  denotes a convolution integral over the incoming quarks transverse momenta, and

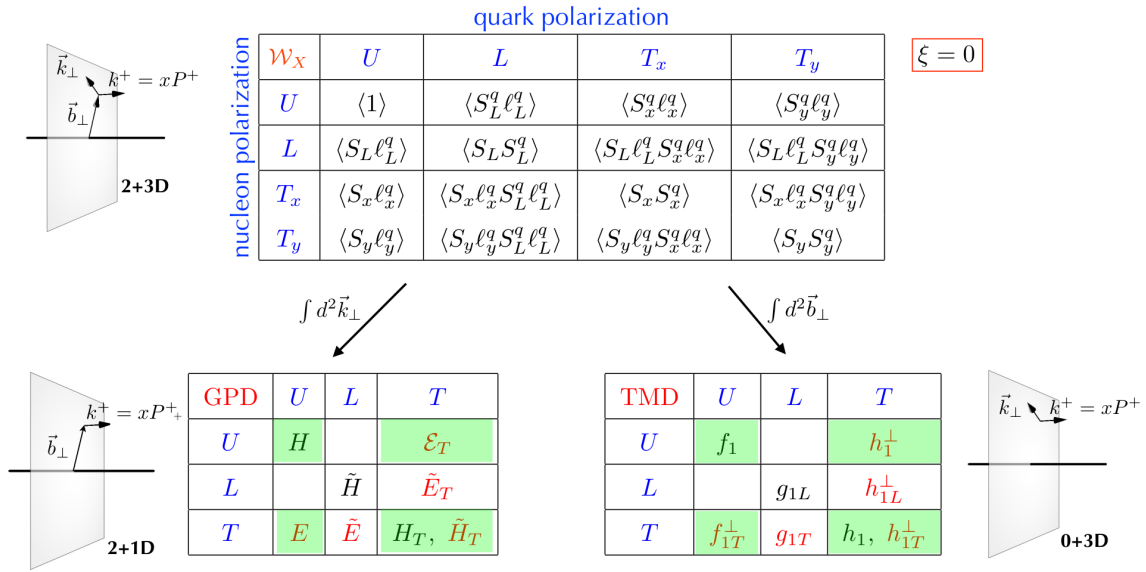


**Fig. 5.** Wigner distributions (top) and leading-twist GPDs and TMDs (bottom) for different combinations of quark and nucleon polarization states. Distributions marked in red vanish for no orbital angular momentum contribution to the nucleon spin, while the quantities highlighted in green can be accessed at LHCspin [13].

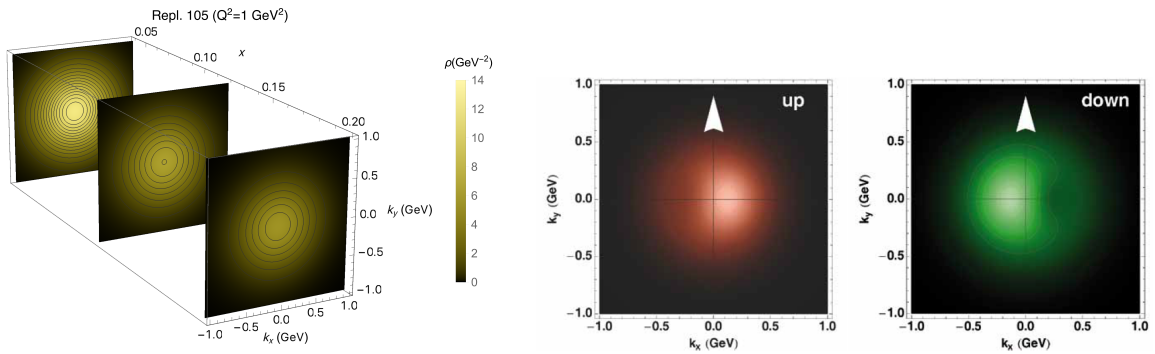


**Fig. 6.** Left: Up quark densities in momentum space [14]. Right: Distortion of the up and down quark distributions in the momentum space when spin is taken into account [15]. These images are elaborated starting from real data and show that the distortion for up- and down-quarks is opposite.

$\phi$  the azimuthal orientation of the lepton pair in the di-lepton centre-of-mass frame. By using a transversely polarized hydrogen (or deuterium) target, one can get sensitivity to the spin-dependent quark TMDs, such as the Sivers function,  $f_1^q(x, p_T^2)$ , and the transversity distribution,  $h_1^q(x, p_T^2)$ , through a Fourier decomposition of the Transverse Single-Spin Asymmetry (TSSA):

$$A_N = \frac{1}{P} \frac{\sigma^\uparrow - \sigma^\downarrow}{\sigma^\uparrow + \sigma^\downarrow} \sim A_{UT}^{\sin(\phi_s)} \sin(\phi_s) + A_{UT}^{\sin(2\phi - \phi_s)} \sin(2\phi - \phi_s) + \dots, \quad (2)$$

where  $P$  denotes the effective target polarization degree (e.g. 80%) and  $\phi_s$  the azimuthal angle of the target transverse polarization with respect to the reaction plane. The azimuthal amplitudes  $A_{UT}^{\sin(\Omega)}$ , with  $\Omega$  representing all relevant combinations of the  $\phi$  and  $\phi_s$  azimuthal angles, constitute the relevant physical observables and provide direct access to combinations of quark TMDs, e.g.:

$$A_{UT}^{\sin(\phi_s)} \sim \frac{f_1^{\bar{q}} \otimes f_{1T}^{\perp,q}}{f_1^{\bar{q}} \otimes f_1^q}, \quad A_{UT}^{\sin(2\phi-\phi_s)} \sim \frac{h_1^{\perp,\bar{q}} \otimes h_1^q}{f_1^{\bar{q}} \otimes f_1^q}, \quad \text{etc.} \quad (3)$$

The transversity distribution, whose knowledge is currently restricted to the valence quarks and to a relatively limited  $x$  region, is extremely interesting not only because it is one of the few TMDs that survive integration over transverse momentum (together with the  $f_1$  and  $g_1$  distributions), but also because a precise determination of its first moment, the tensor charge, could allow to set stringent constraints to physics beyond the Standard Model [16]. Being T-odd, it is theoretically established that the Sivers and the Boer-Mulders functions extracted in DY must have opposite sign with respect to the same quantities extracted in semi-inclusive deep inelastic scattering (SIDIS) [17]. This fundamental QCD prediction can be verified by exploiting the large sample of DY data expected at LHCspin. In addition, isospin effects can be investigated by comparing p-H and p-D collisions. Projections for DY measurements evaluated at the LHCb fixed-target kinematics and based on an integrated luminosity of  $10 \text{ fb}^{-1}$  are shown in Fig. 7 [18].

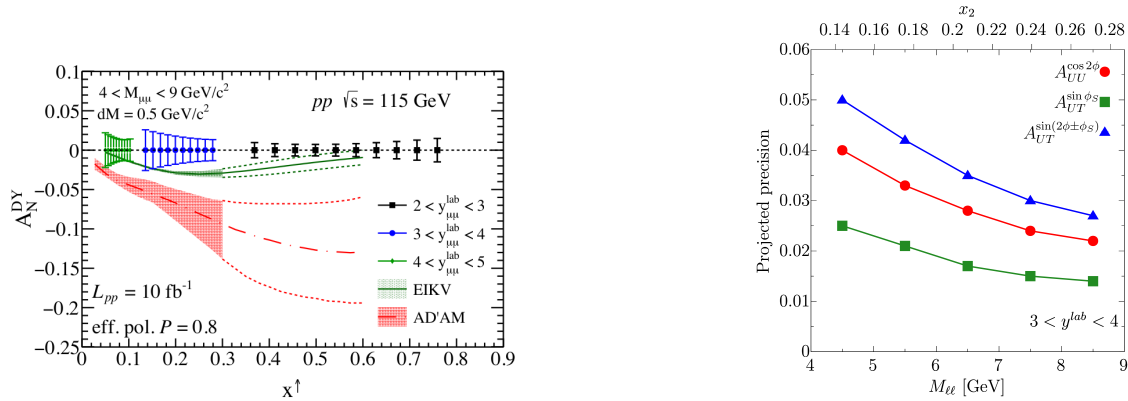


**Fig. 7.** Left: projections of  $A_N$  as a function of  $x$  for DY events at the LHCb fixed-target kinematics compared to theoretical predictions. Right: projected precision for selected azimuthal asymmetry amplitudes with DY data in a specific rapidity interval, as a function of the di-lepton invariant mass [18].

Besides providing access to the quark TMDs, by using both H and D targets, the DY process also allows to study the anti-quark content of the nucleon. LHCspin can in fact potentially complement, at a different kinematics, the recent intriguing results of the SeaQuest/E906 experiment [19], which show a clear excess of the unpolarized *anti-down* quark distribution compared to the *anti-up* one, demonstrating that the proton sea is far from being flavour symmetric and much more complex than originally thought. Similar measurements could, in principle, be already anticipated with SMOG2.

### 3.1.2 gluon TMDs

While first phenomenological extractions of quark TMDs have been performed in recent years, based mainly on SIDIS data, gluon TMDs are presently essentially unknown. Measurements of observables sensitive to gluon TMDs, such as, e.g., the gluon Sivers function [20], represent nowadays the new frontier of this research field. Since, at LHC, heavy quarks are mainly produced via gluon-gluon fusion, production of quarkonia and open heavy-flavour states represents the most efficient way to study the gluon dynamics inside nucleons and to probe the gluon TMDs. Specifically, by measuring inclusive production of  $J/\psi$ ,  $\psi'$ ,  $D^0$ ,  $\eta_c$ ,  $\chi_c$ ,  $\chi_b$ , etc., for which LHCb is well suited and optimized, using the high-energy and high-intensity LHC proton beams in conjunction with a transversely polarized H or D target, LHCspin has the potential to become a unique facility for these studies.

While the unpolarized  $f_1^g$  and the Boer-Mulders  $h_1^{\perp,g}$  gluon TMDs can be accessed through the study of the azimuthal dependence of the cross section, the gluon TMDs that require a transversely polarized nucleon, such as the gluon Sivers function  $f_{1T}^{\perp,g}$ , can be probed through a Fourier decomposition of the TSSA:

$$A_N = \frac{1}{P} \frac{\sigma^{\uparrow} - \sigma^{\downarrow}}{\sigma^{\uparrow} + \sigma^{\downarrow}} \propto [f_1^g(x_b, p_{T,b}) \otimes f_{1T}^{\perp,g}(x_t, p_{T,t}) \otimes d\sigma_{gg \rightarrow QQg}] \sin(\phi_s) + \dots, \quad (4)$$

where  $d\sigma_{gg \rightarrow QQg}$  denotes the elementary hard-scattering cross-section, calculable in perturbative QCD, and the indices  $b$  and  $t$  the beam and the target proton, respectively. Figure 8 (left) shows the  $x_F$  dependence of two model predictions for  $A_N$  in inclusive  $J/\psi$  events [21]. Asymmetries as large as 5-10 % could be expected in the negative  $x_F$  region, where the LHCspin sensitivity is highest.

Since transverse-momentum-dependent QCD factorization requires  $p_T(Q) \ll M_Q$ , where  $Q$  denotes a heavy quark, the safest inclusive processes to be studied with a polarized hydrogen target is associated quarkonium production, e.g.:

$$pp^{\uparrow} \rightarrow J/\psi + J/\psi + X, \quad pp^{\uparrow} \rightarrow J/\psi + \psi' + X, \quad pp^{\uparrow} \rightarrow \Upsilon + \Upsilon + X, \quad \text{etc.}, \quad (5)$$

where only the relative  $p_T$  has to be small compared to  $M_Q$ . Asymmetries as large as 5 % are predicted as a function of the relative  $p_T$  for the  $\cos(2\phi)$  and  $\cos(4\phi)$  modulations of the unpolarized cross-section for quarkonium-pair production [22], as shown in Fig. 8.

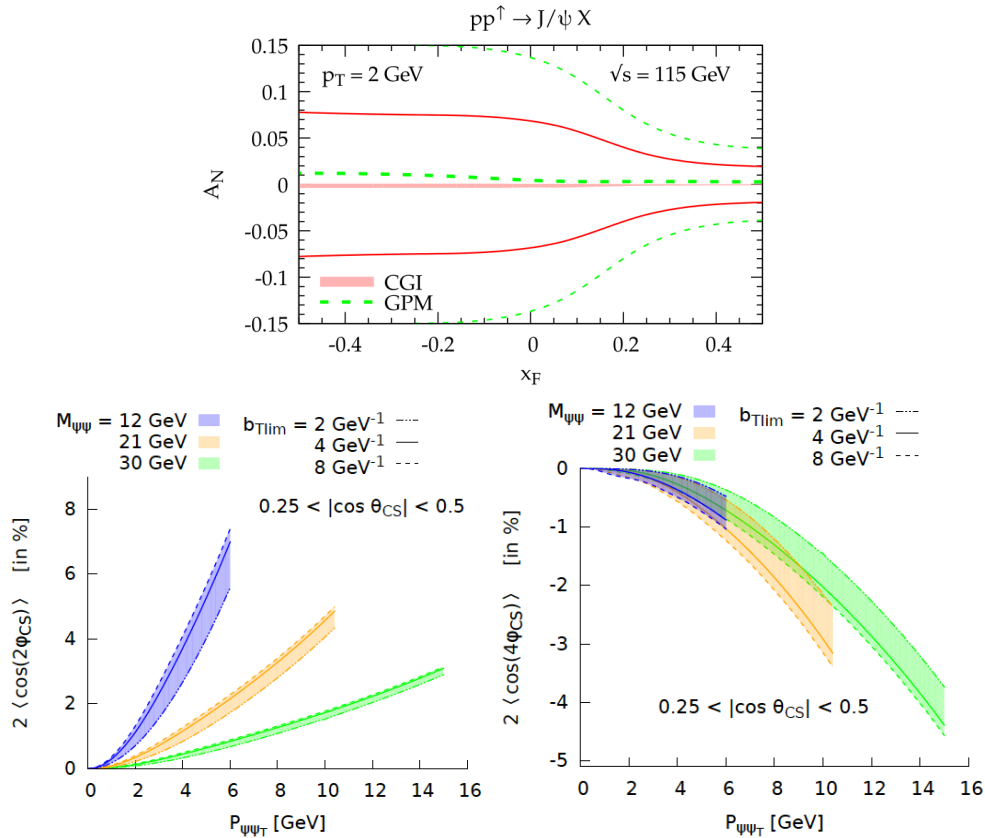


**Fig. 8.** Top: theoretical predictions for  $A_N$  in inclusive  $J/\psi$  production [21]. Bottom: theoretical predictions for the  $\cos(2\phi)$  (left) and  $\cos(4\phi)$  (right) asymmetry amplitudes of the unpolarized cross section for di- $J/\psi$  production as a function of the relative transverse momentum [22].

### 3.1.3 GPDs

While TMDs provide a “tomography” of the nucleon in momentum space (Fig. 6, left), complementary 3D maps can be obtained in the spatial coordinate space by measuring GPDs (Fig. 9 left). Correlating transverse position and longitudinal momentum, GPDs provide an access to the parton orbital angular momentum, whose contribution to the total nucleon spin can be inferred via the Ji sum rule [23]. The essentially unknown gluon GPDs can be experimentally probed at LHC in exclusive quarkonia production in Ultra-Peripheral Collisions (UPCs), which are dominated by the electromagnetic interaction, in events where a pomeron exchange with the target nucleon occurs [24] (Fig. 9 right). First measurements of  $J/\psi$  production in UPC in PbPb collisions have recently been reported by the LHCb collaboration [25]. With the LHCspin polarized target, TSSAs in UPCs can be exploited to access, e.g., the  $E_g$  GPD, which has never been measured so far and represents a key element of the proton spin puzzle.

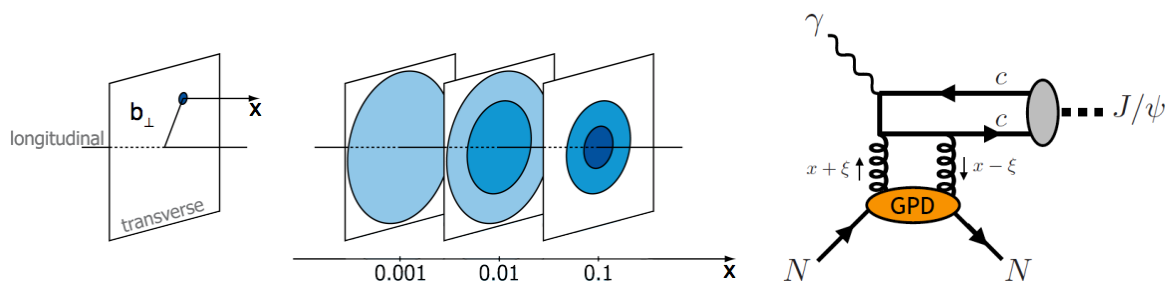


**Fig. 9.** Left: Nucleon tomography in coordinate space. Right: Access to gluon GPDs in UPC.

### 3.1.4 Heavy ion collisions

An interesting topic joining heavy-ion and spin physics is the study of collective phenomena in heavy-light systems through ultrarelativistic collisions of heavy nuclei with transversely polarized deuterons. Polarized deuteron targets offer, in fact, a unique opportunity to control the orientation of the formed fireball by measuring the elliptic flow relative to the polarization axis (ellipticity). The spin 1 deuteron nucleus is prolate (oblate) in the  $j_3 = \pm 1$  ( $j_3 = 0$ ) configuration, where  $j_3$  is the projection of the spin along the polarization axis. The deformation of the target deuteron can influence the orientation of the fireball in the transverse plane, as shown in Fig. 10. The measurement proposed in [26] can be performed at LHCspin exploiting the high-intensity LHC heavy-ion beams.

### 3.2 The experimental setup

The R&D of the LHCspin setup points at the development of a new generation Polarized Gas Target (PGT). The starting point of the R&D is the polarized target system employed at the HERMES experiment [9], and comprises three main components: an Atomic Beam Source (ABS), a Storage Cell (SC), and a diagnostic system. The ABS consists of a dissociator with a cooled nozzle, a Stern-Gerlach apparatus to focus the wanted hyperfine states, and adiabatic RF-transitions for setting and switching the target polarization between states of opposite sign. The ABS injects a beam of polarized hydrogen or deuterium into the SC, which is located in the LHC primary vacuum along the beam pipe section upstream of the VELO. The SC, based on the same concept of the SMOG2 one, is located inside a vacuum chamber and surrounded by a compact superconductive dipole magnet, as shown in Fig. 11 left. The magnet generates a 300 mT static transverse field with a homogeneity of 10 % over the full volume of the cell, which is necessary to maintain the transverse polarization of the gas inside the cell, and to avoid beam-induced depolarization [27]. Studies for the inner coating of the SC are



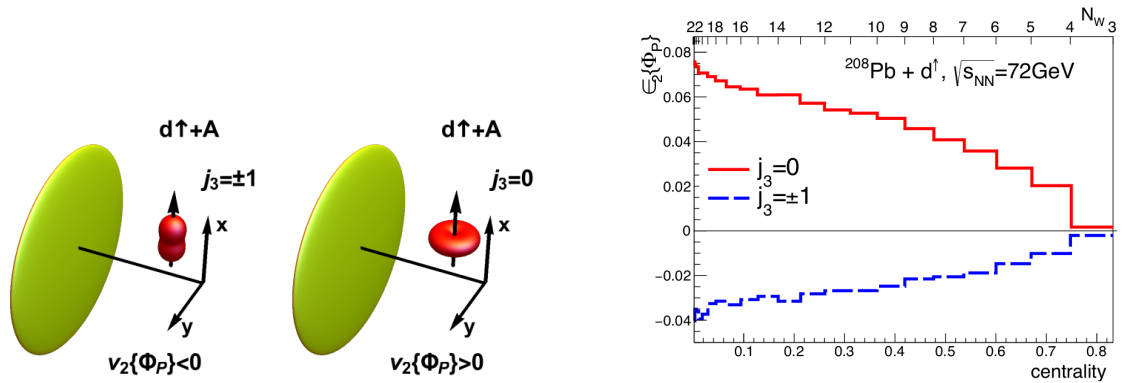


**Fig. 10.** Left: sketch of a ultra-relativistic collision of a lead nucleus against a transversely polarized deuteron in two different angular momentum projections. Right: ellipticity with respect to the polarization axis as a function of the collision centrality with LHCspin kinematics [26].

currently ongoing, with the aim of producing a surface that minimizes the molecular recombination rate as well as the secondary electron yield. The diagnostic system continuously analyses gas samples drawn from the SC and comprises a target gas analyzer to detect the molecular fraction, and thus the degree of dissociation, and a Breit-Rabi polarimeter to measure the relative population of the injected hyperfine states. The entire setup installed in the VELO alcove is sketched in Fig. 11 right.

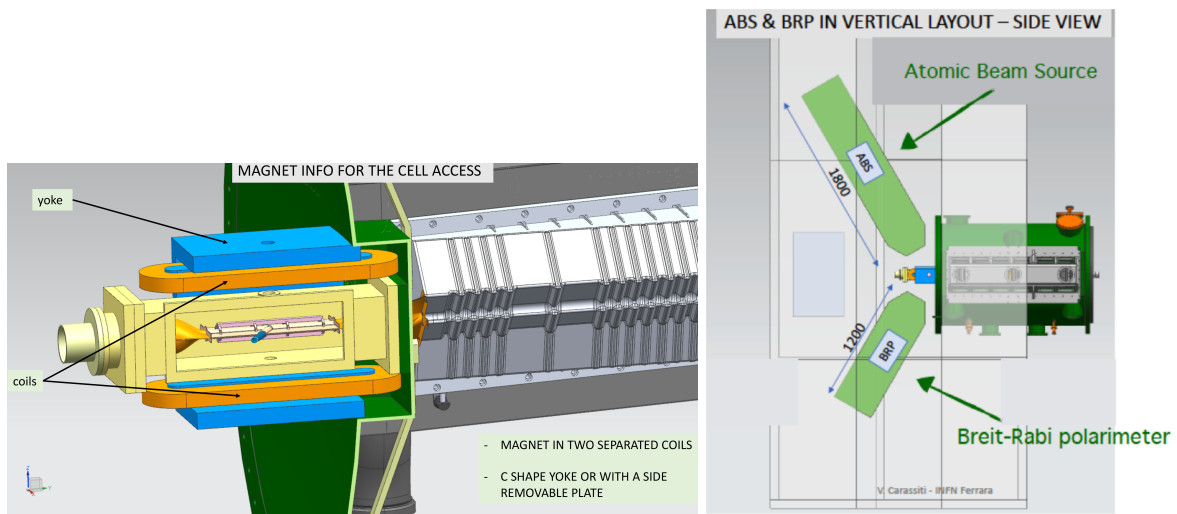


**Fig. 11.** Left: A drawing of the LHCspin vacuum chamber (yellow) hosting the storage cell. The chamber is inserted between the coils of the magnet (orange) and the iron return yoke (blue). The VELO vessel and RF box are shown in green and grey, respectively. Right: sketch of the full setup installed in the VELO alcove.

Figure 12 shows the efficiency to reconstruct a primary vertex and both tracks in simulated  $\Upsilon \rightarrow \mu^+\mu^-$  events as a function of  $x_F$  for three different positions of the SC. The simulation is performed using the upgraded LHCb detector geometry. New algorithms are currently being developed for the Run 3 fixed-target reconstruction and are expected to sensibly improve the current performance as well as to enable to record LHCspin data in parallel with beam-beam collisions. An instantaneous luminosity of  $O(10^{32}) \text{ cm}^{-2} \text{ s}^{-1}$  is foreseen for fixed-target p-H collisions in Run 4, with a further factor 3-5 increase for the high-luminosity LHC phase from Run 5 (2032).

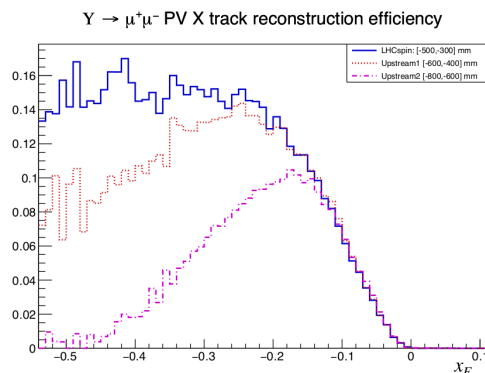


**Fig. 12.** Simulated reconstruction efficiency for  $\Upsilon \rightarrow \mu^+\mu^-$  events for three different storage cell positions. The blue line, corresponding to the SMOG2 storage cell location, is shown for reference.

## 4. Conclusions

The fixed-target physics program at LHC has been greatly enhanced with the recent installation of the SMOG2 setup at LHCb. LHCspin is the natural evolution of SMOG2 and aims at installing a polarized gas target to bring spin physics at LHC for the first time, opening a whole new range of exploration. With strong interest and support from the international theoretical community, LHCspin is a unique opportunity to advance our knowledge on several unexplored QCD areas, complementing both existing facilities and the future Electron-Ion Collider [28].

## References

- [1] LHCb Collaboration, A. A. Alves Jr. *et al.*, JINST **3**, S08005 (2008).
- [2] LHCb Collaboration, R. Aaij *et al.*, CERN-LHCC-2011-001, LHCC-I-018, (2011).
- [3] LHCb Collaboration, R. Aaij *et al.*, JINST **9**, P12005 (2014), arXiv:1410.0149.
- [4] LHCb Collaboration, R. Aaij *et al.*, Phys. Rev. Lett. **121**, 222001 (2018), arXiv:1808.06127.
- [5] LHCb Collaboration, R. Aaij *et al.*, Phys. Rev. Lett. **122**, 132002 (2019), arXiv:1810.07907.
- [6] LHCb Collaboration, SMOG2 Upgrade Tech. Rep., CERN-LHCC-2019-005, LHCB-TDR-020 (2019).
- [7] LHCb Collaboration, <https://cds.cern.ch/record/2688875>.
- [8] C. A. Aidala *et al.*, arXiv:1901.08002.
- [9] HERMES Collaboration, A. Airapetian *et al.*, Nucl. Instrum. Meth. A **540**, 68 (2005) physics/0408137.
- [10] ANKE Collaboration, M. mikirtychyants *et al.*, arXiv:1212.1840 [physics.ins-det].
- [11] A. Bursche *et al.*, Document for Physics Beyond Collider CERN WG, LHCb-PUB-2018-015 (2019).
- [12] S. Bhattacharya *et al.*, Phys. Lett. B **771**, 396 (2017), [Erratum: Phys.Lett.B 810, 135866 (2020)].
- [13] <https://indico.bnl.gov/event/9726/contributions/47605/attachments/33594/54332/DIS2021-Pasquini.pdf>.
- [14] A. Bacchetta *et al.*, JHEP **06**, 081 (2017), arXiv:1703.10157. [Erratum: JHEP 06, 051 (2019)].
- [15] A. Bacchetta and M. Contalbrigo, Il Nuovo Saggiatore **28**, 16 (2012).
- [16] A. Courtoy *et al.*, Phys. Rev. Lett. **115**, 162001 (2015), arXiv:1503.06814.
- [17] J. C. Collins, Phys. Lett. B **536**, 43 (2002), hep-ph/0204004.
- [18] C. Hadjidakis *et al.*, arXiv:1807.00603.
- [19] J. Dove, B. Kerns, R.E. McClellan *et al.*, Nature **590**, 561 (2021).
- [20] D. Boer *et al.*, Advances in High Energy Physics **10**, 024 (2015), arXiv:1504.04332 [hep-ph].
- [21] U. D' Alesio *et al.*, Phys. Rev. D **99**, no. 3 036013 (2019), arXiv:1811.02970.
- [22] F. Scarpa *et al.*, EPJ C **80**, 87 (2020).
- [23] X.-D. Ji, Phys. Rev. Lett. **78**, 610 (1997), hep-ph/9603249.
- [24] J. Koempel *et al.*, Phys. Rev. D **85**, 051502 (2012).
- [25] LHCb Collaboration, A. Bursche *et al.*, Nuclear Physics A **982**, 247 (2019).
- [26] W. Broniowski and Božek, Phys. Rev. C **101**, no. 2 024901 (2020), arXiv:1906.09045.
- [27] Steffens *et al.*, PoS SPIN2018 (2019) 098, arXiv:1901.06361.
- [28] A. Accardi *et al.*, Eur. Phys. J. A **52**, no. 9 268 (2016), arXiv:1212.1701.